Acta Biomaterialia 9 (2013) 8983–8990

Contents lists available at SciVerse ScienceDirect

Acta Biomaterialia

journal homepage: www.elsevier.com/locate/actabiomat

In vivo acute and humoral response to three-dimensional porous soy protein scaffolds

Karen B. Chien [a,b], Brian A. Aguado [b,c], Paul J. Bryce [d], Ramille N. Shah [a,b,e,*]

[a] Department of Materials Science and Engineering, Northwestern University, Evanston, IL 60208, USA
[b] Institute for BioNanotechnology in Medicine, Northwestern University, Chicago, IL 60611, USA
[c] Department of Biomedical Engineering, Northwestern University, Evanston, IL 60208, USA
[d] Division of Allergy–Immunology, Feinberg School of Medicine, Northwestern University, Chicago, IL 60611, USA
[e] Department of Surgery, Feinberg School of Medicine, Northwestern University, Chicago, IL 60611, USA

ARTICLE INFO

Article history:
Received 7 May 2013
Received in revised form 17 June 2013
Accepted 2 July 2013
Available online 12 July 2013

Keywords:
In vivo
Soy protein
Scaffolds
Biocompatibility
Subcutaneous

ABSTRACT

Increasing interest in using soy biomaterials for tissue engineering applications has prompted investigation into the in vivo biocompatibility of soy implants. In this study, the biocompatibility of soy protein scaffolds fabricated using freeze-drying and 3-D printing was assessed using a subcutaneous implant model in BALB/c mice. The main objectives of this study were: (1) to compare soy protein with bovine collagen, a well-characterized natural protein implant, by implanting scaffolds of the same protein weight, and (2) to observe the effects of soy scaffold microstructure and amount of protein loading, which also alters the degradation properties, on the acute and humoral immune responses towards soy. Results showed that freeze-dried soy scaffolds fully degraded after 14 days, whereas collagen scaffolds (of the same protein weight) remained intact for 56 days. Furthermore, Masson's trichrome staining showed little evidence of damage or fibrosis at the soy implant site. Scaffolds of higher soy protein content, however, were still present after 56 days. H&E staining revealed that macrophage infiltration was hindered in the denser bioplotted soy scaffolds, causing slower degradation. Analysis of soy-specific antibodies in mouse serum after implantation revealed levels of IgG_1 that correlated with higher scaffold weight and protein density. However, no soy-specific IgE was detected, indicating the absence of an allergic response to the soy implants. These results demonstrate that soy protein could be an acceptable biocompatible implant for tissue regeneration, and that scaffold porosity, soy protein density and scaffold degradation rate significantly affect the acute and humoral immune response.

© 2013 Acta Materialia Inc. Published by Elsevier Ltd. All rights reserved.

1. Introduction

Soy protein is a natural, renewable and abundant resource readily extracted and isolated from whole soybeans. Versatility in soy protein processing has fueled interest in using this material for tissue engineering [1,2] and wound healing [3,4] applications. Initial evaluations of soy as a biocompatible biomaterial *in vitro* have established that cells remain viable when seeded on soy structures [5–7] or when soy is dissolved in cell culture media [8]. Soy protein membranes prepared by casting solutions of soy protein in water and air-drying passed both direct contact (scanning electron microscopy (SEM) observation) and indirect contact (Dulbecco's modified Eagle medium extraction and MTT viability) biocompatibility assays using L929 mouse fibroblasts [5]. Human mesenchymal stem cells have been shown to adhere and proliferate *in vitro* on porous soy protein scaffolds fabricated through freeze-drying and three-dimensional (3-D) printing [6,7]. Soy granules made from defatted soy (containing soy protein) have been shown to stimulate the synthesis of collagen [9] and mineralized bone noduli [8] *in vitro*, as well as promote the formation of trabecular bone in a femoral critical sized defect *in vivo* [10]. The inherent bioactivity of soy and the achievable range of structural and mechanical properties with soy structures [6,7,11] demonstrate that soy can be a promising biomaterial for a variety of tissue engineering targets.

Soy protein contains all essential and non-essential amino acids including cysteine [12]. Cysteines allow for disulfide bonding during heat treatment, which can affect protein solubility and mechanical properties of casted products [12]. Soy has unique intermolecular and intramolecular forces, allowing for a wide range of gelation properties [13]. Hydrogen bonds, disulfide bonds and hydrophobic interactions resulting from the molecular structure of soy are necessary for the formation and maintenance of 2-D and 3-D stable structures [6,13]. Studies from the food and

* Corresponding author at: Institute for BioNanotechnology in Medicine, Northwestern University, Chicago, IL 60611, USA. Tel.: +1 312 503 3931; fax: +1 312 503 2482.
E-mail address: ramille-shah@northwestern.edu (R.N. Shah).

1742-7061/$ - see front matter © 2013 Acta Materialia Inc. Published by Elsevier Ltd. All rights reserved.
http://dx.doi.org/10.1016/j.actbio.2013.07.005

biomedical industries have demonstrated that soy protein materials can be fabricated into a variety of structures with varying properties, including films [14–16], hydrogels [17] and scaffolds [6,7]. Therefore, soy protein serves as an ideal material for studying the effects of scaffold microstructure on the biological response *in vitro* and *in vivo*.

As with any novel material being developed as an implant, there is a demand for further biocompatibility characterization of soy protein structures *in vivo*. This is particularly relevant in the case of soy, since spontaneous allergy to soy affects 0.4% of children; the levels of soy-specific IgE are predictive of disease progression [18]. To date, the *in vivo* biocompatibility of soy has mostly been explored with soy as a composite material mixed with other natural materials such as chitosan [19] and cellulose [20] in the form of membranes and sponges. In this study, the safety of implanting soy protein scaffolds fabricated by freeze-drying and 3-D printing was assessed with two main objectives. The first objective was to compare soy protein with collagen, a commonly used FDA-approved natural protein implant material. The second objective was to observe the effects of scaffold microstructure and amount of protein loading, which also alters the degradation properties, on the immune response towards soy. These 3-D porous soy protein scaffolds were hypothesized to be degradable with resolvable inflammation levels by tuning the open porosity of the scaffolds, which can also promote cell infiltration and better integration of the scaffold with surrounding tissue.

2. Materials and methods

2.1. Fabrication of freeze-dried collagen and soy scaffolds

Soy protein isolate containing 87.6% protein (Solae LLC, St Louis, MO) as determined by the combustion method [21] was used for this study. Both 1 and 3 wt.% soy protein slurries were formed by mixing with glycerol (1:1 weight ratio to soy protein) in MQ water. Glycerol was added as a biocompatible plasticizer specifically required for the soy scaffold fabrication process to achieve porous structures [7]. Solutions were homogenized for 5 min, and the 1% and 3% solutions were casted into 7 cm aluminum dishes in volumes of 13 ml and 30 ml, respectively to achieve scaffolds of similar weight when punched with a 6 mm punch. Collagen slurries were fabricated by dissolving 1 wt.% bovine type I collagen (Sigma–Aldrich, St Louis, MO) in 0.05 M acetic acid (Sigma–Aldrich) and homogenizing for at least 30 min until all protein was dissolved. Slurries were vacuumed until all air pockets were removed, and 25 ml of the slurry was casted into 7 cm aluminum dishes. Upon casting, all slurries were immediately lyophilized in an AdVantage BenchTop lyophilizer (VirTis, Gardiner, NY) using a procedure described previously [7]. Briefly, slurries were frozen at a rate of $-0.5\ ^{\circ}C\ min^{-1}$ down to $-15\ ^{\circ}C$ and held at temperature for 5 h, then dried at a pressure of 100 mtorr for at least 2 days. All freeze-dried scaffolds were punched using a 6 mm biopsy punch. The weights of the scaffolds were measured prior to surgery preparations. Soy scaffolds of 1 and 3 wt.% with weights of 1.65 ± 0.1 and 14 ± 0.5 mg were chosen for surgeries. The heights of 1% collagen scaffolds were trimmed using micro-scissors to achieve equivalent weight for comparison with 1% soy scaffolds.

2.2. Fabrication of bioplotted soy scaffolds

Slurries consisting of 20 wt.% soy protein and 4 wt.% glycerol in MQ water were fabricated and printed into 3-D scaffolds with controlled pore size and geometry using the Bioplotter (EnvisionTEC GmbH, Germany) employing a previously described method [6]. Briefly, the mixed slurries were sieved sequentially through autoclaved 297 μm and 105 μm pore size sieves and printed through a 200 μm needle with inter-strut spacing of 400 μm. Every other layer was rotated 90°, with a lateral shift of 0.5 mm every four layers to achieve an overlapping conformation to minimize through pores and enhance cell seeding efficiency. Scaffolds were fabricated to the given height of 12 layers with a layer spacing of 250 μm to achieve equivalent weight for comparison with 3% soy protein freeze-dried scaffolds (14 ± 0.5 mg).

2.3. Characterization of scaffold structure using SEM and porosimetry

SEM was performed using a LEO Gemini 1525 FEG SEM with an acceleration voltage of 15 kV (Oberkochen, Germany) to observe and compare the microstructure of the various scaffolds. Scaffolds were coated with 10 nm of osmium using an osmium plasma coater (Filgen, Structure Probe, West Chester, PA) prior to imaging. A mercury intrusion porosimeter (Micromeritics, Norcross, GA) was used to determine the volume percent porosity and pore size diameter distributions for all groups ($N = 3$) using a previously described method [22].

2.4. Implantation of 3-D scaffolds

Scaffolds were immersed in 70% ethanol for at least 12 h and soaked in phosphate buffered saline (PBS, HyClone, Logan, UT) overnight prior to surgery. Female BALB/c mice age 6–8 weeks were used for this study ($N = 6$ per group per time point, 96 mice total). Mice were anesthetized using isoflurane, and a 5–6 mm incision was made on the shaved dorsal side. Forceps were used to create a subcutaneous pocket in which one scaffold was placed per mouse. Non-absorbable nylon sutures were used to close the incision site. Mice were killed at days 1, 14, 28 and 56 after scaffold implantation. The surgical protocol followed NIH guidelines for the care and use of laboratory animals and was approved by Northwestern University's Animal Care and Use Committee (Chicago, IL, USA).

2.5. Assessment of implant degradation

The size of the implants in the mice was measured using digital calipers every 3 days after surgery. The implant volume was assumed to be the cylindrical area underneath the skin. The thickness of the scaffold (h) was measured, and the diameter of the implant under the skin (d) was measured three times and averaged. The implant volume was calculated using the formula $\pi \cdot (d/2)^2 \cdot h$ and observed for all mice with a palpable implant.

2.6. Histology of implanted scaffolds

Subcutaneous implants were excised and fixed in 10% neutral buffered formalin. Control tissue was obtained by excising an isolated area of the lower dorsal side of a mouse that had no contact with the implant. Tissues were dehydrated using graded ethanol solutions and embedded in paraffin wax. The samples were sectioned into 4 μm thick sections. Sections were deparaffinized, rehydrated and stained using routine hematoxylin and eosin (H&E) stain and Masson's trichrome stain.

2.7. Evaluation of serum immunoglobulin levels using ELISA

Naive mice ($N = 5$) were immunized with 100 μl soy protein (10 μg) with aluminum hydroxide adjuvant (3 mg) on days 0 and 7 and sacrificed at day 14, to establish a reference sera pool for comparing serum from implanted mice for all assays performed. Sera of scaffold implanted mice were collected at each time point, and the soy-specific antibody levels were detected using enzyme-

linked immunosorbent assay (ELISA). 96-well flat bottom, high binding plates (Immulon II; Nunc, Roskilde, Denmark) were coated with 10 mg ml^{-1} soy protein solubilized in carbonate buffer overnight at 4 °C. Between additions of all reagents, plates were rinsed three times in 0.05% Tween-20 in PBS. Plates were blocked using 3% bovine serum albumin (BSA, Sigma–Aldrich) for 2 h at room temperature. Samples and standards were added to the blocked plates. The pooled reference sera were assigned an arbitrary unit value that was used as a standard for all assays performed. All samples were diluted in 3% BSA in PBS and analyzed in duplicate. Samples were incubated overnight at 4 °C. Biotin-labeled secondary antibodies against murine IgG_1, IgG_3, IgM and IgE (3 μg ml^{-1}) were added and incubated for 1 h at room temperature. Horseradish peroxidase-conjugated streptavidin (1:1000 dilution, Invitrogen, Carlsbad, CA) was applied for signal amplification, and after 30 min, ABTS substrate (1:100 dilution, Invitrogen) was added. Absorbance was read at 405 nm after color development. Sample relative units werecalculated based on the linear regime of the arbitrary units generated by the standard curve ($R^2 > 0.9$) from pooled sera of immunized mice.

2.8. Statistical analysis

Statistics were performed using SPSS (Chicago, IL). Groups were compared using independent Student's *t*-test, with *P*-values <0.05 considered statistically significant.

3. Results

3.1. Fabrication of collagen and soy 3-D porous scaffolds

Comparative collagen (1% Col-FD) and soy protein (1% Soy-FD) scaffolds were successfully fabricated using the same freeze-drying protocol. The resulting scaffold microstructures had non-homogeneous pore structures at the surface; the pores were spread throughout the scaffold thickness as observed in the cross-sectional SEM images (Fig. 1A–D). Bioplotted soy scaffolds (Soy-BP) had dense struts with widths between 200 and 300 μm, and globular protein structures were visible on the strand surface (Fig. 1E). The cross-section of the bioplotted scaffold revealed pockets of air within the strands and uneven distribution of pores due to collapse of the soft material structure in the *z*-direction during fabrication (Fig. 1F). To compare scaffolds fabricated using different methods, freeze-dried scaffolds with weight similar to the bioplotted scaffolds (14 mg) were generated by using a slurry with a higher starting soy concentration (3% Soy-FD). The resulting scaffolds had a more densely packed porous structure at the surface and throughout the cross-section (Fig. 1G and H).

Total percent porosity and pore size distributions were quantified using mercury intrusion porosimetry (Fig. 2). The pore size distribution for collagen scaffolds was spread uniformly across the range of pore diameters measured. Both soy protein freeze-dried scaffold groups had a narrower distribution of pore sizes, with 1% and 3% soy scaffolds having the largest volume percent of pore sizes, ~60 μm and 16 μm, respectively (Fig. 2A). Bioplotted scaffolds had a peak in total pore volume at a pore size of 5 μm due to the grooves on the printed strand surfaces, and since the printed pore structure was interconnected, the pore size distribution was skewed between 150 and 300 μm. The total porosity of the scaffolds was significantly different ($P < 0.05$) between the scaffolds of 1.6 mg and 14 mg weights regardless of material or fabrication procedure (Fig. 2B).

3.2. Degradation of scaffolds in the subcutaneous pocket

All implanted scaffolds placed in the subcutaneous pocket on the dorsal side of the mouse degraded over time with minimal scarring and no infections. Measuring scaffold size and estimating the implant volume over time allowed for the comparison of degradation rates between scaffold groups. The only group with 100% of scaffolds degraded was the 1% soy scaffold group, where one mouse had a fully degraded scaffold by day 15 and all scaffolds were degraded by day 18 (Fig. 3). The collagen scaffolds (1% Col-FD) and the higher concentrated freeze-dried soy protein scaffolds (3% Soy-FD) had similar starting implant volumes and degradation rates even though the loaded protein weights were different, and both groups had at least one mouse with a completely degraded scaffold after 33 days (Fig. 3). Although the bioplotted soy scaffold had a similar starting implant volume as the collagen and 3% soy scaffold, there was an increased implant volume within the first 2 weeks of implantation before the implant volume decreased, and all of the scaffolds were still evident by 2 months (Fig. 3). Macroscopic observations of the implant site showed that there were no visible deformities induced as a result of implantation, and skin and hair growth appeared normal (Fig. 3).

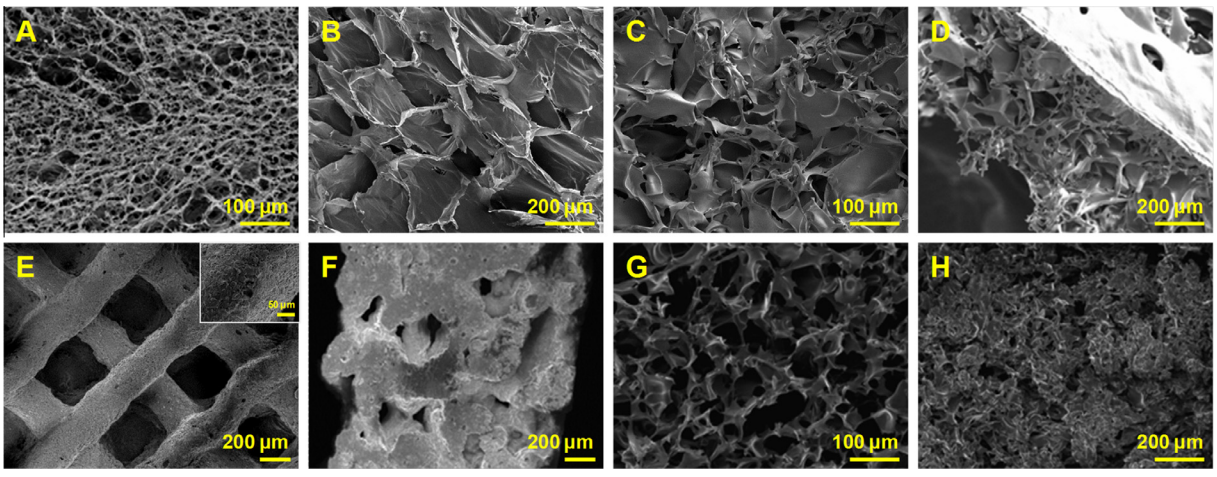

Fig. 1. Representative SEM images of the top and cross-section surfaces of various scaffolds. (A, B) 1 wt.% freeze-dried collagen scaffolds. (C, D) 1 wt.% freeze-dried soy scaffolds. (E, F) Bioplotted soy scaffolds. (G, H) 3 wt.% freeze-dried soy scaffolds. (A, C, E, G) Top surface of scaffold. (B, D, F, H) Cross-section surface of the scaffold. Inset in (E) is a representative zoom-in image of the bioplotted strand surface.

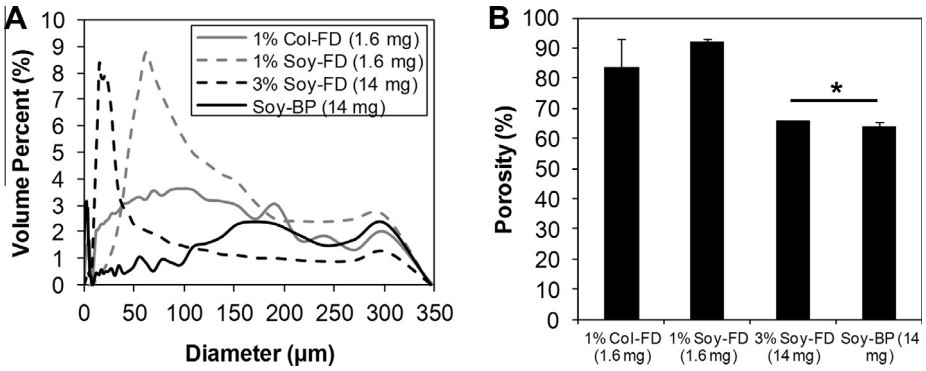

Fig. 2. Porosity characterization of the various scaffolds. (A) Representative pore size distribution of scaffolds. Col: collagen, FD: freeze-dried, BP: bioplotted. (B) Total percentage of occupied pore space within scaffolds ($N = 3$, error bars = ±1 SD). $^{*}P < 0.05$.

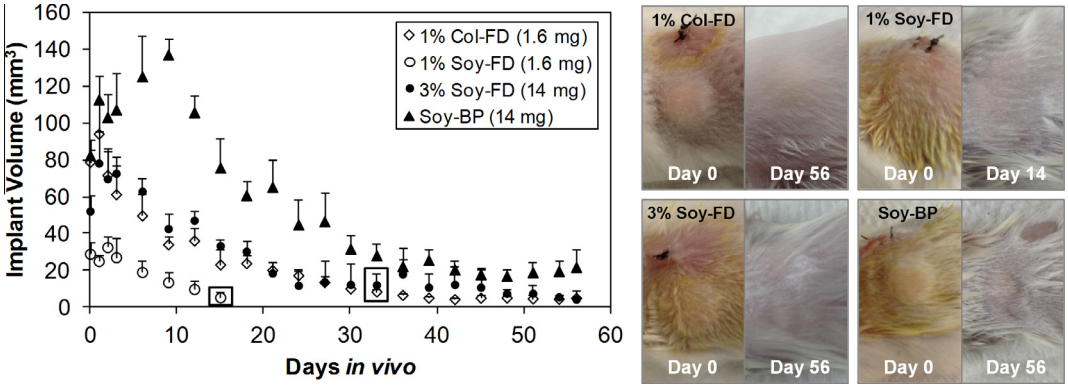

Fig. 3. Degradation of various scaffolds *in vivo* (left) characterized by implant volume ($N = 3$–6 per data point, positive error bars = 1 SD) and macroscopic view of implants on the dorsal side of the mouse (right). Col: collagen, FD: freeze-dried, BP: bioplotted. Dorsal area was shaved prior to images being acquired. Boxes in the chart denote the first time points in which at least one mouse had a fully degraded (non-visible) scaffold. This was day 15 for 1% Soy-FD and day 33 for both 1% Col-FD and 3% Soy-FD. No scaffolds were fully degraded for the Soy-BP group.

3.3. Comparison of acute immune response between soy and collagen scaffolds

Since the soy protein implants were not rejected from any of the mice, we examined if there was any evidence of acute immune responses. A comparison of H&E-stained tissue sections from the local implant site of collagen and soy freeze-dried scaffolds with equal weight protein loading demonstrated that the initial inflammatory response was similar (Fig. 4). Neutrophils (dark nuclear staining) were seen infiltrating the scaffold and forming a fibrous capsule barrier immediately at day 1. Interestingly, cells appeared to have infiltrated the entire soy protein scaffold but not the collagen scaffold, as indicated by the cellular stains present throughout the soy scaffold but appearing only on the outer rim of the collagen scaffold (Fig. 4). The interface of the scaffold and the growing fibrous capsule appeared similar, with neutrophils gathering within the pores. At day 14, the soy protein scaffolds were mostly degraded, while neutrophils were still invading the collagen scaffold, and were progressing to penetrate deeper towards the center of the scaffold (Fig. 4).

To investigate the local effect of the quickly degrading 1% freeze-dried soy scaffolds (1% Soy-FD), the efficacy of healing at the implantation site after full scaffold degradation was assessed using Masson's trichrome staining. The collagenous fibrous capsule was observed over time (Fig. 5). At day 1, the formation of a thin fibrous capsule containing a high density of neutrophils was visualized at the interface between the scaffold and the epidermis/muscle. No remnants of soy protein scaffold were found after 14 days; a thicker fibrous capsule was observed where the scaffold was originally. After 1 month and beyond, however, the implant sites remodeled and appeared normal and similar to control tissue. This result suggests that soy protein scaffolds can fully degrade with no lingering local responses at the implantation site.

3.4. Comparison of acute immune response between freeze-dried and bioplotted soy scaffolds

Since there were differences in degradation, the local immune response to higher weight freeze-dried and bioplotted soy protein scaffolds were examined using H&E staining at 1, 14, 28 and 56 days after implantation. The higher weight freeze-dried scaffolds seemed to induce an initial response similar to the lower weight freeze-dried scaffolds; at day 1 after implantation of 3% freeze-dried soy scaffolds, neutrophils were beginning to infiltrate the scaffold (Fig. 6). After 2 weeks, a thicker fibrous capsule was observed. The capsule persisted in size after 28 days, and signs of resolution were evident by day 56. The scaffold appeared to be broken down into precipitates at 28 days. Magnified images of the cell–scaffold interfaces showed the protein scaffold of the freeze-dried structure breaking apart over the time course of the study. Macrophages were identified after 14 days, with an increasing number at the site up to 56 days. The scaffold appeared to be degrading from the outside to the inside, with eosin staining revealing buildup of inflammatory tissue surrounding macrophages and the degraded protein remnants (Fig. 6). At all time points, lymphocytes were observed within the scaffolds, and clusters of neutrophils were identified at the junctions between the scaffold protein and the neighboring skin or muscle.

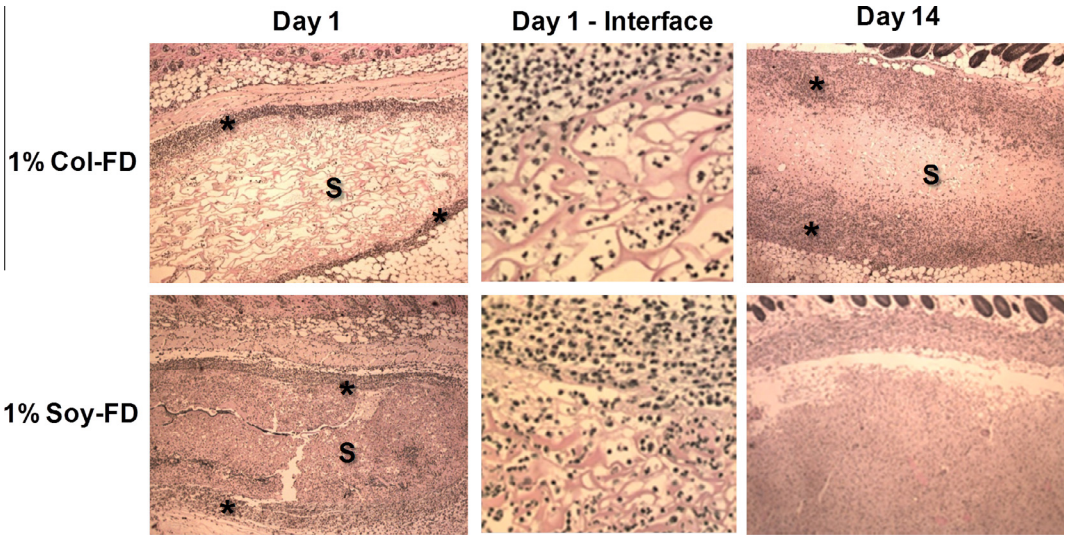

Fig. 4. Comparison of 1% freeze-dried collagen and soy scaffolds at days 1 and 14 using H&E staining. Col: collagen, FD: freeze-dried. Orientation of images from top to bottom is epidermis to subcutaneous tissue, with scaffold implanted subcutaneously (5 × magnification for days 1 and 14, 40 × magnification for the imaging showing the interface between the scaffold and the fibrous capsule). The scaffold was fully degraded at day 14 for the 1% Soy-FD group. S: scaffold; *: fibrous capsule.

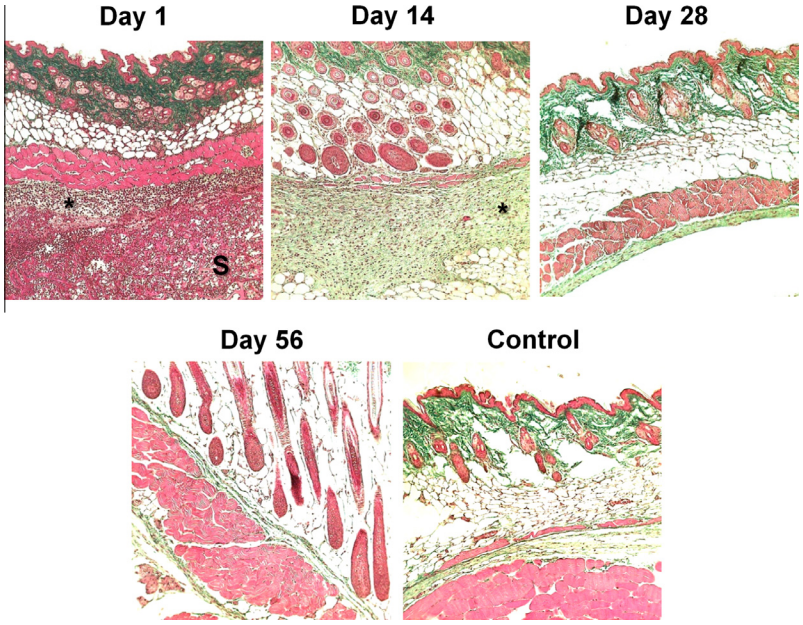

Fig. 5. Quick degradation of 1% freeze-dried soy protein scaffolds (1% Soy-FD) at days 1, 14, 28 and 56 after implantation as observed using Masson's Trichrome stain (10×) to visualize the fibrous capsule area. Healing of tissue to normal state and reduction of fibrous capsule size was observed after 28 days. S: scaffold; *: fibrous capsule.

A similar early neutrophil and late macrophage response was observed for the bioplotted soy scaffolds (Fig. 7). The initial response at day 1 for the bioplotted scaffolds involved clustering of neutrophils at the surface of the implant and within pockets of the bioplotted pore structures. Since scaffold density was higher compared to freeze-dried scaffolds, the cell infiltration was less homogeneous, with cells settling in the grooves of the globular structures on the strand surfaces. However, the bioplotted scaffold also eroded from the outer struts inwards, with greater density of neutrophils at the dense scaffold surface and macrophage clusters around the degraded protein remnants towards the epidermis. After 2 weeks, macrophages were detected and dispersed throughout the implant area with diminished neutrophil populations. Globular pieces of soy protein scaffold surrounded by inflammatory cells were observed to have broken away from the main bioplotted structure. Further erosion of the main structure was observed after 1 month, with a higher density of macrophages compared to neutrophils. After 2 months, the entire protein structure was degraded into globular pieces which were surrounded by proteinaceous debris serving as a matrix holding together a greater number of macrophages with fewer neutrophils compared to previous time points.

3.5. Humoral response to soy protein scaffolds

To observe the systemic response to the implanted soy protein scaffolds, the soy-specific antibody levels in the sera of implanted mice were quantified and normalized to antibody levels in immunized mice sera. IgM, IgG_1 and IgG_3 isotypes were detected (Fig. 8), while IgE (indicative of an allergic response) was not. Baseline

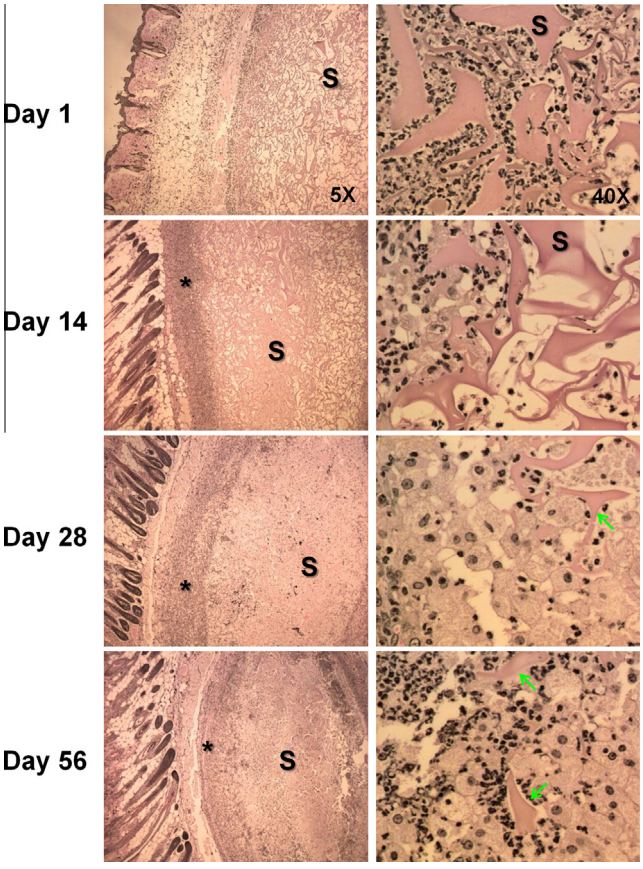

Fig. 6. Comparison of 3% freeze-dried scaffold implants (3% Soy-FD) at 1, 14, 28 and 56 days after implantation. Orientation of images from left to right is epidermis to subcutaneous tissue, with scaffold implanted subcutaneously. Within each group and time point, the image on the left was taken at 5×, and the image on the right was taken at 40×. S: scaffold; *: fibrous capsule. Arrows point to degraded soy protein scaffolds.

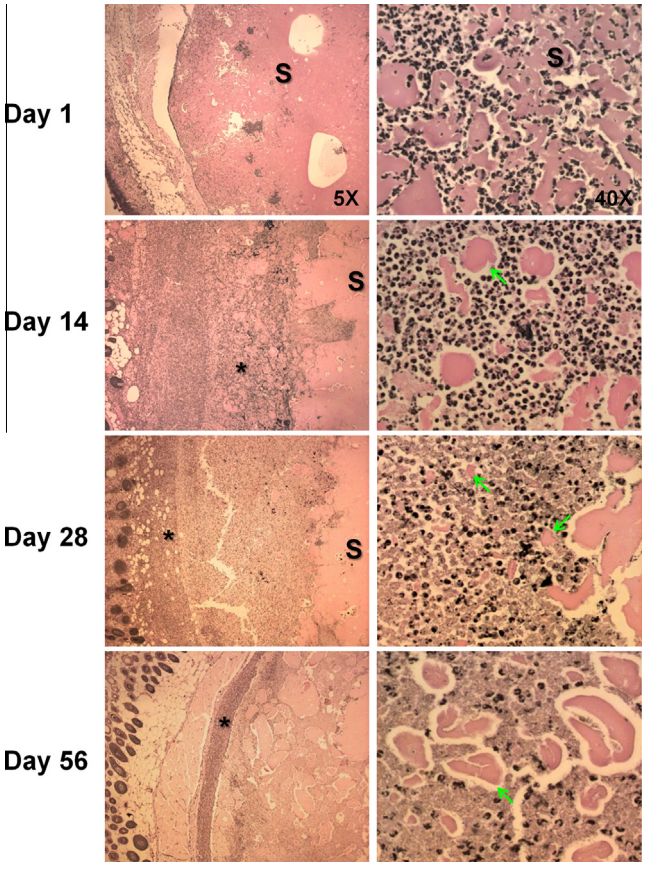

Fig. 7. Comparison of bioplotted scaffold implants (Soy-BP) at 1, 14, 28 and 56 days after implantation. Orientation of images from left to right is epidermis to subcutaneous tissue, with scaffold implanted subcutaneously. Within each group and time point, the image on the left was taken at 5×, and the image on the right was taken at 40×. S: scaffold; *: fibrous capsule. Arrows point to degraded soy protein scaffolds.

levels of IgM and IgG_1 were detected in mice with no implant (143.6 ± 31.8 RU ml^{-1} and 426.4 ± 178.0 RU ml^{-1}), and IgG_3 antibodies were detected in one of the non-implanted mice (245.6 RU ml^{-1}). Levels of IgM rose significantly between controls and day 1 for all groups ($P < 0.05$). After implantation, IgM levels were significantly different between day 1 and 56 for the 1% freeze-dried soy group ($P < 0.005$) and between day 14 and 28 for the 3% freeze-dried soy group ($P < 0.05$, Fig. 8A). There was a significant increase in IgG_1 levels between controls and day 1 ($P < 0.005$) and day 1 and 14 for all groups ($P < 0.05$, Fig. 8B). The mean level of IgG_1 was greater for the bioplotted soy scaffolds compared to the 3% freeze-dried scaffolds loaded at equivalent protein weight ($P = 0.0547$), with highly variable antibody levels for the bioplotted group at both days 28 and 56 (greater than 1×10^6 RU ml^{-1}variability) that caused an increase in the standard error of the mean (SEM). Mean IgG_3 levels were increased over time (Fig. 8C), with significant increases in 1% soy scaffolds from day 1 to 14 and from days 14 and 28 to day 56 (all $P < 0.05$). There was a significant increase in IgG_3 levels for 3% soy scaffold between day 1 and day 28 ($P < 0.01$) and an increase for the bioplotted scaffolds from day 1 to day 14 ($P < 0.001$) and between day 14 and day 56 ($P < 0.05$).

4. Discussion

Ideal tissue engineering platforms require material and structural properties specific to their particular application. Soy protein is a versatile material that can be processed using various methods to create different 3-D structures. In this study, freeze-dried and 3-D printed soy scaffolds were fabricated and characterized for their material and biological properties. Analysis of microstructure and architecture using SEM and porosimetry demonstrated that pore size distributions and surface textures could be manipulated (Figs. 1 and 2). In comparison to 1 wt.% freeze-dried collagen scaffolds, 1 wt.% freeze-dried soy scaffolds possessed a similar percent porosity of ~90%. However, pore sizes of the 1% freeze-dried soy scaffolds was better controlled with a greater cumulative percent volume of pores between 100 and 300 μm (Fig. 2), which is an ideal range for tissue engineering applications to allow for a sufficient number of binding sites (through exposed surface area) while still allowing for cell ingrowth and nutrient diffusion [23]. Percent porosity was decreased for higher weight freeze-dried and bioplotted soy scaffolds as expected (Fig. 2B). The main benefit of using 3-D printing for fabrication is that pore sizes can be designed and controlled; in this case, bioplotting of soy helped to increase the volume percent of pore sizes greater than 100 μm (Fig. 2A).

This study was the first to directly compare soy and collagen scaffolds *in vivo* for tissue engineering applications. Since porosity and degradation rate of scaffolds can significantly affect the *in vivo* response, a comparison of soy scaffolds fabricated with different protein weight percentages and fabrication techniques was also performed. No immune rejection occurred when soy scaffolds were implanted subcutaneously in mice. In fact, when lesser amounts of protein were implanted (1% Soy-FD), the scaffolds were fully degraded after 14 days (Fig. 3) with similar appearance to control tis-

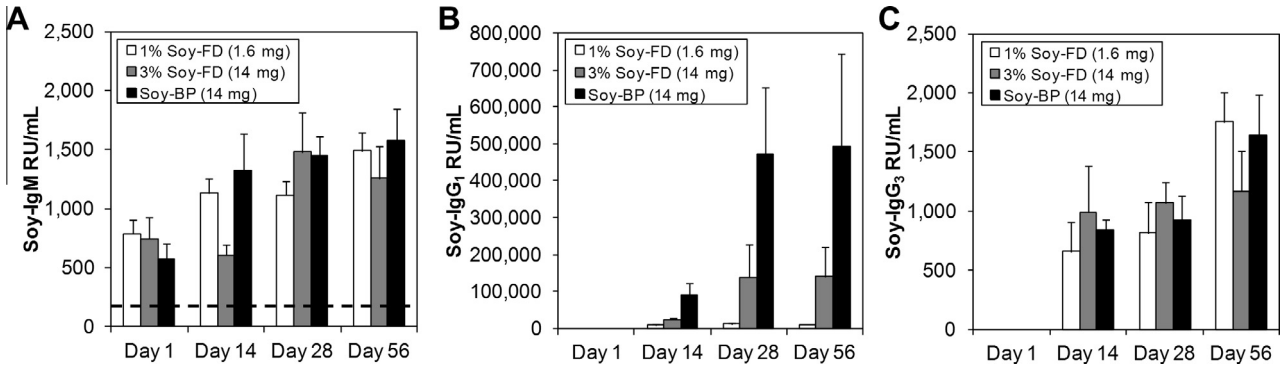

Fig. 8. Specific antibody response to implanted (FD: freeze-dried, BP: bioplotted) soy protein scaffolds over 56 days ($N = 6$, error bars = ± SEM). (A) Relative production of soy-specific IgM. Dotted line represents baseline level of IgM in non-implanted mice (143.6 ± 31.8 RU ml^{-1}). (B) Relative production of soy-specific IgG_1. Baseline level of IgG_1 was observed (426.4 ± 178.0 RU ml^{-1}). (C) Relative production of soy-specific IgG_3. Non-implanted mice had no baseline level of IgG_3.

sue at the final time point (56 days). Although the implant site increased in size for the bioplotted soy scaffolds (Soy-BP), indicating swelling or a greater inflammatory response compared to the other groups, the skin around the implant healed completely and the scaffold size steadily decreased after two weeks. This is an indication that wound healing occurred and the initial inflammatory response resolved over time. Our results for collagen scaffold degradation times and acute immune response coincided with observations reported previously for bovine collagen type I/III sponges subcutaneously implanted in rats [24]. In a direct comparison between soy and collagen scaffolds, the fibrous capsule formation was of similar thickness throughout time (Fig. 4). The local resolution of the implant is a classic, non-specific wound healing response [25,26], which is shown to be similar to collagen scaffold degradation with the same amount of protein added. Observations of the implant over time through H&E and Masson's trichrome staining (Figs. 4 and 5) showed that complete local healing can occur upon implantation of a soy protein scaffold.

Higher weight freeze-dried and bioplotted soy scaffolds were also chosen for *in vivo* evaluation. The main purpose for testing these groups was to determine the biocompatibility of the bioplotted scaffolds, which can produce scaffolds with a greater range of properties, and to compare the immune response to the freeze-dried scaffolds. Another purpose was to observe the immune response in the presence of higher protein content, which can also significantly affect the degradation of the scaffold *in vivo*. Unlike with the 1% freeze-dried scaffolds, neutrophils continued to remain at the site of 3% freeze-dried scaffolds after 56 days, indicating more persistent inflammation (Fig. 6). A similar pattern was observed for the bioplotted scaffolds (Fig. 7). Although inflammation was more severe with higher weight soy scaffolds, the loss of implant volume over time for both the bioplotted and 3 wt.% freeze-dried soy scaffold groups indicated that the inflammation was constantly resolving starting after two weeks (Fig. 3) as the scaffolds degraded. The bioplotted scaffolds resulted in larger and denser soy fragments that were more difficult to break down *in vivo*, which most likely resulted in the more severe response. This may potentially be alleviated by freeze-drying a bioplotted soy scaffold after printing in order to instill a more porous structure within the struts of the scaffold; this would decrease the density of the scaffold struts and facilitate *in vivo* degradation. Overall, examination of the implant site over two months demonstrated that the degradation rate of soy protein scaffolds and the density of the scaffold features can significantly influence the local inflammatory response.

Since these scaffolds are protein based, it is important to assess the extent of any humoral immune response over time. IgM, IgG_1 and IgG_3 were detected and increased over time for all three implant groups (Fig. 8). Soy protein presentation to B cells caused increased antibody production, resulting in continuous recruitment of immune cells to the implant site until the scaffold is completely dissolved. Class switching from IgM to IgG_1 and IgG_3 was observed after 14 days, with a steady continuous increase in IgM. The average IgG_1 levels increased three orders of magnitude for both higher weight scaffolds (3% Soy-FD and Soy-BP). This increase would have been significant between the bioplotted scaffolds and the two freeze-dried groups, but the range of antibody responses varied greatly for the bioplotted scaffolds (with one value $>1 \times 10^6$), resulting in a higher SEM ($P < 0.06$ between bioplotted scaffolds at day 28 and day 56 compared to all other groups). This result implies that a greater density of lingering soy scaffold could increase systemic IgG_1 levels. It is important to note that baseline levels of IgG_1 and IgM were also detected in control mice receiving no implant, likely a consequence of soy in the mouse feed used in this study. It was previously reported that dietary antigens can cause a weak antibody response but no adverse immune responses because oral tolerance processes was retained [27,28]. Although significant increases of all antibody isotypes were observed after 2 months of scaffold implantation (Fig. 8), mice were able to continue tolerating a soy-rich diet with no allergic symptoms or tendencies and never progressed to generate soy specific-IgE.

Soy protein scaffolds show promise as a versatile natural biomaterial implant for tissue engineering applications. Soy scaffolds can be easily fabricated using different types of fabrication techniques [2], as well as further modified via enzymatic [7] or chemical cross-linking. Depending on the tissue target, implanting lower amounts of soy protein can achieve faster degradation rates with decreased soy-specific humoral immune response. The results from this study indicate a less severe immune response to soy biomaterials compared to previously reported subcutaneous implantation of soy protein membranes [19]. This can be attributed to the open porous design of the scaffolds which allowed cells to infiltrate into the matrix and more readily degrade the protein. The acute immune response for 1% freeze-dried soy scaffolds was not only comparable to collagen scaffolds of the same protein content, but also to porcine small intestinal submucosa-based scaffolds at 2 weeks [29]. These scaffolds were also better integrated at 28 days compared to zein (corn based protein) scaffolds [30] and appeared more biocompatible than cotton implants that resulted in severe inflammation [31]. Further investigation will involve testing soy protein biomaterials in more functional applications to evaluate the degradation kinetics and biological response at other implant sites.

5. Conclusion

The structural properties of soy protein scaffolds can be altered by using different fabrication processes. From this, the effect of soy

scaffold weight, porosity and degradation rate on the local and systemic immune response were evaluated in a subcutaneous implant over two months. A comparison of freeze-dried soy and collagen implants of the same weight showed that the acute immune response was similar. When the soy scaffold was fully degraded, the inflammation at the local site of implantation was completely resolved. The severity of the immune response was greater with increased amount of protein loading, lower porosity and slower degradation rate. This result reiterates the importance of considering the amount of material loading, scaffold microstructure and scaffold degradation kinetics in tissue engineering. These factors affect the immune response and could potentially alter the functionality of the material. Although increased levels of soy-specific antibodies were detected after scaffold implantation over time, no allergy-related IgE was detected over the time frame of the study, and animals remained orally tolerant to soy in their diet. Overall, these results show promise in being able to use porous soy protein scaffolds as biomaterial implants for regenerative medicine applications if optimal scaffold characteristics (i.e. protein density, porosity, degradation) are achieved.

Acknowledgments

This work was funded with a National Science Foundation Graduate Research Fellowship awarded to K.B.C. Soy protein was obtained from Solae, LLC as part of a Materials Transfer Agreement; Solae performed the combustion test to determine protein content. Mercury intrusion porosimetry results were performed on a porosimeter graciously provided by Dr. Katherine Faber (Northwestern University). Northwestern University Electron Probe Instrumentation Center provided sample preparation and SEM imaging. The Equipment Core Facility at the Institute for BioNanotechnology in Medicine at Northwestern University (NU) graciously provided use of lyophilizers and sample preparation tools. This work was also supported by the Northwestern University Mouse Histology and Phenotyping Laboratory and a Cancer Center Support Grant (NCI CA060553), with many thanks to Dr. Li Lin for her support and guidance.

Appendix A. Figures with essential colour discrimination

Certain figures in this article, particularly Figs. 3-7 are difficult to interpret in black and white. The full colour images can be found in the on-line version, at doi: http://dx.doi.org/10.1016/j.actbio.2013.07.005

References

[1] Malafaya PB, Silva GA, Reis RL. Natural-origin polymers as carriers and scaffolds for biomolecules and cell delivery in tissue engineering applications. Adv Drug Deliv Rev 2007;59:207–33.
[2] Santin M, Ambrosio L. Soybean-based biomaterials: preparation, properties and tissue regeneration potential. Expert Rev Med Devices 2008;5:349–58.
[3] Peles Z, Zilberman M. Novel soy protein wound dressings with controlled antibiotic release: mechanical and physical properties. Acta Biomater 2012;8:209–17.
[4] Peles Z, Binderman I, Berdicevsky I, Zilberman M. Soy protein films for wound-healing applications: antibiotic release, bacterial inhibition and cellular response. J Tissue Eng Regen Med 2012;7:401–12.
[5] Silva GA, Vaz CM, Coutinho OP, Cunha AM, Reis RL. In vitro degradation and cytocompatibility evaluation of novel soy and sodium caseinate-based membrane biomaterials. J Mater Sci Mater Med 2003;14:1055–66.
[6] Chien KB, Makridakis E, Shah RN. Three-dimensional printing of soy protein scaffolds for tissue regeneration. Tissue Eng C 2012;19:417–26.
[7] Chien KB, Shah RN. Novel soy protein scaffolds for tissue regeneration: material characterization and interaction with human mesenchymal stem cells. Acta Biomater 2012;8:694–703.
[8] Santin M, Morris C, Standen G, Nicolais L, Ambrosio L. A new class of bioactive and biodegradable soybean-based bone fillers. Biomacromolecules 2007;8:2706–11.
[9] Meikle ST, Standen G, Salvage J, De Santis R, Nicolais L, Ambrosio L, et al. Synthesis and characterization of soybean-based hydrogels with an intrinsic activity on cell differentiation. Tissue Eng A 2012;18:1932–9.
[10] Merolli A, Nicolais L, Ambrosio L, Santin M. A degradable soybean-based biomaterial used effectively as a bone filler in vivo in a rabbit. Biomed Mater 2010;5:15008.
[11] Vaz CM, de Graaf LA, Reis RL, Cunha AM. In vitro degradation behaviour of biodegradable soy plastics: effects of crosslinking with glyoxal and thermal treatment. Polym Degrad Stab 2003;81:65–74.
[12] Shimada K, Cheftel JC. Determination of sulfhydryl groups and disulfide bonds in heat-induced gels of soy protein isolate. J Agric Food Chem 1988;36:147–53.
[13] Utsumi S, Kinsella JE. Forces involved in soy protein gelation: effects of various reagents on the formation, hardness and solubility of heat-induced gels made from 7S, 11S, and soy isolate. J Food Sci 1985;50:1278–82.
[14] Brandenburg AH, Weller CL, Testin RF. Edible films and coatings from soy protein. J Food Sci 1993;58:1086–9.
[15] Chen L, Remondetto G, Rouabhia M, Subirade M. Kinetics of the breakdown of cross-linked soy protein films for drug delivery. Biomaterials 2008;29:3750–6.
[16] Ogale AA, Cunningham P, Dawson PL, Acton JC. Viscoelastic, thermal, and microstructural characterization of soy protein isolate films. J Food Sci 2000;65:672–9.
[17] Maltais A, Remondetto GE, Subirade M. Soy protein cold-set hydrogels as controlled delivery devices for nutraceutical compounds. Food Hydrocolloid 2009;23:1647–53.
[18] Savage JH, Kaeding AJ, Matsui EC, Wood RA. The natural history of soy allergy. J Allergy Clin Immunol 2010;125:683–6.
[19] Santos TC, Marques AP, Silva SS, Oliveira JM, Mano JF, Castro AG, et al. Chitosan improves the biological performance of soy-based biomaterials. Tissue Eng *Pt* A 2010;16:2883–90.
[20] Luo LH, Zhang YF, Wang XM, Wan Y, Chang PR, Anderson DP, et al. Preparation, characterization, and in vitro and in vivo evaluation of cellulose/soy protein isolate composite sponges. J Biomater Appl 2010;24:503–26.
[21] AOAC. Official Methods of Analysis of AOAC International, 17th edn. Gaithersburg, MD:AOAC International; 2000.
[22] Pappacena KE, Gentry SP, Wilkes TE, Johnson MT, Xie S, Davis A, et al. Effect of pyrolyzation temperature on wood-derived carbon and silicon carbide. J Eur Ceram Soc 2009;29:3069–77.
[23] Freyman TM, Yannas IV, Gibson LJ. Cellular materials as porous scaffolds for tissue engineering. Prog Mater Sci 2001;46:273–82.
[24] Anselme K, Bacques C, Charriere G, Hartmann DJ, Herbage D, Garrone R. Tissue reaction to subcutaneous implantation of a collagen sponge. A histological, ultrastructural, and immunological study. J Biomed Mater Res 1990;24:689–703.
[25] Remes A, Williams DF. Immune response in biocompatibility. Biomaterials 1992;13:731–43.
[26] Martin P, Leibovich SJ. Inflammatory cells during wound repair: the good, the bad and the ugly. Trends Cell Biol 2005;15:599–607.
[27] Husby S. Normal immune responses to ingested foods. J Pediatr Gastroenterol Nutr 2000;30:S9–S13.
[28] Christensen HR, Brix S, Frokiaer H. Immune response in mice to ingested soya protein: antibody production, oral tolerance and maternal transfer. Br J Nutr 2004;91:725–32.
[29] Kim MS, Ahn HH, Shin YN, Cho MH, Khang G, Lee HB. An in vivo study of the host tissue response to subcutaneous implantation of PLGA- and/or porcine small intestinal submucosa-based scaffolds. Biomaterials 2007;28:5137–43.
[30] Wang HJ, Gong SJ, Lin ZX, Fu JX, Xue ST, Huang JC, et al. In vivo biocompatibility and mechanical properties of porous zein scaffolds. Biomaterials 2007;28:3952–64.
[31] Hickey T, Kreutzer D, Burgess DJ, Moussy F. In vivo evaluation of a dexamethasone/PLGA microsphere system designed to suppress the inflammatory tissue response to implantable medical devices. J Biomed Mater Res 2002;61:180–7.